Chinese Chemical Letters 37 (2026) 112429

Contents lists available at ScienceDirect

Chinese Chemical Letters

journal homepage: www.elsevier.com/locate/cclet

Shape-persistent hexa(ethynylpyridine) macrocycles as adaptive hosts for cations

Pengfei Niu[a,b], Jiawei Ma[c], Beijing Zhang[a,b], Ziyao Nie[a,b], Haitao Liu[a,b], Yong Liang[c], Xing Jiang[a,b,*]

[a] South China Advanced Institute for Soft Matter Science and Technology School of Emergent Soft Matter, South China University of Technology, Guangzhou 510640, China
[b] Guangdong Provincial Key Laboratory of Functional and Intelligent Hybrid Materials and Devices, South China University of Technology, Guangzhou 510640, China
[c] School of Chemistry and Chemical Engineering, Nanjing University, Nanjing 210023, China

ARTICLE INFO

Article history:
Received 1 August 2025
Revised 14 January 2026
Accepted 18 January 2026
Available online 14 April 2026

Keywords:
Shape-persistent macrocycles
Endo-functionalization
Adaptive
Host–guest chemistry
Sonogashira reaction

ABSTRACT

We present the synthesis and host-guest complexation of endo-functionalized shape-persistent hexa(ethynylpyridine) macrocycles (Py_6MCs). The challenging macrocyclization of linear hexapyridine precursors was achieved by using catalytic amount of $PdCl_2(PPh_3)_2$ and stoichiometric CuI in the Sonogashira reaction, or with K_2CO_3 as an additive under copper-free conditions. Single-crystal X-ray diffraction revealed that Py_6MCs with different side chains all feature a near-planar framework, with notable flexibility to adopt chair-like or boat-like conformations. The polar and electron-rich cavities of Py_6MCs render them attractive hosts for cationic guests. ^1H NMR and fluorescence titrations showed that Py_6MC1 and Py_6MC2 formed 1:1 complexes with *N*-methyl pyridinium and quaternary ammonium cations, and high affinity (up to 3.1×10^5 L/mol) was achieved for cations of distinct shapes and sizes. Density functional theory (DFT) calculations showed that Py_6MC readily deforms to complement the structures of different guests, demonstrating a high level of adaptivity.

© 2026 Published by Elsevier B.V. on behalf of Chinese Chemical Society and Institute of Materia Medica, Chinese Academy of Medical Sciences.

The pursue of new host molecules has been an everlasting theme in supramolecular chemistry since Pedersen's seminal report of crown ethers [1]. Shape-persistent macrocycles feature cavities of well-defined geometry, and are hence poised to bind guests of complementary size and shape [2–8]. Their host-guest complexation can be enhanced by endo-functionalization, *i.e.,* introducing sites of interaction inside the cavity [9–15]. A facile approach to achieve endo-functionalization of shape-persistent macrocycles is to replace benzene moieties with pyridines, as the inward pointing nitrogen can participate in hydrogen bonds and other intermolecular interactions [16–20]. Tobe prepared butadiyne-bridged pyridinophane **1** (Fig. 1), which forms host-guest complexes with tropylium cation [21]. Inouye reported pyridine macrocycle **2** with acetylene and butadiyne linkers, which binded β-maltoside with high selectivity [22,23]. Hexa(ethynylenepyridylene) macrocycle Py_6MC has been a desired host molecule with a moderate-sized polar cavity suitable for binding electron-deficient guests. However, the high electron density inside the macrocycle has rendered Py_6MC synthetically challenging. Previous attempts to prepare Py_6MC by cyclization of linear precursors such as **3** failed [24]. Acyclic polymers were obtained instead, partially due to unfavored dipole interactions in the "closed" conformation (Fig. S1 in Supporting information). Herein, we report the successful synthesis of three Py_6MCs with different substituents by using catalytic amount of $PdCl_2(PPh_3)_2$ and stoichiometric CuI, or with K_2CO_3 as an additive in a copper-free condition in the ring-closing Sonogashira reaction. Their crystal structures suggested that Py_6MC1–3 could adopt planar and non-planar conformations, and that their cavities are occupied by polar ethylene glycol side chains or water molecules in the solid state. ^1H NMR and fluorescence titrations suggested that Py_6MCs form 1:1 complexes with pyridinium and quaternary ammonium cations in solution, with association constants (K_a) up to 3.1×10^5 L/mol. We were surprised to find that comparable K_a values were obtained for multiple cationic guests despite their differences in size and shape, which suggested notable adaptivity of Py_6MCs. DFT calculations confirmed that cations are bound in the macrocycle cavity by C–H···N hydrogen bonds and analogous weak interactions. Host-guest interactions led to notable distortion of Py_6MC to fit guests of different structural features.

* Corresponding author.
E-mail address: xingj@scut.edu.cn (X. Jiang).

https://doi.org/10.1016/j.cclet.2026.112429
1001-8417/© 2026 Published by Elsevier B.V. on behalf of Chinese Chemical Society and Institute of Materia Medica, Chinese Academy of Medical Sciences.

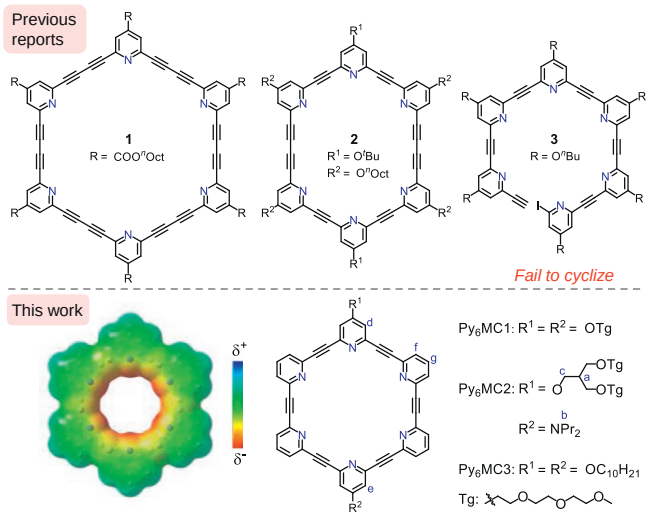
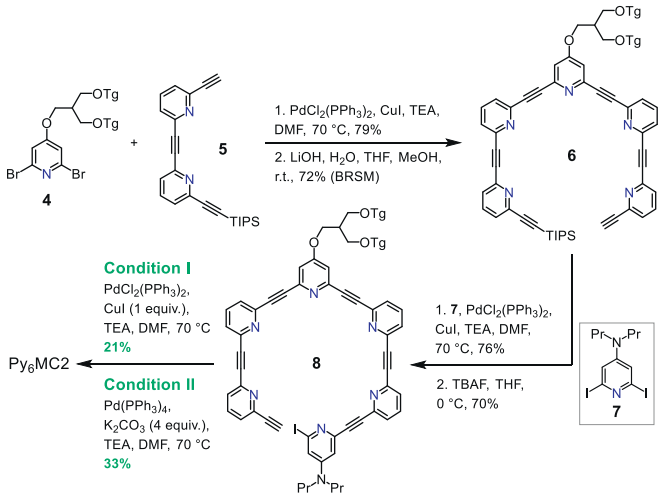


Fig. 1. Alkyne-bridged pyridine oligomers in literature (top). Electrostatic potential map of Py_6MC and Py_6MC1-Py_6MC3 in this work (bottom).



Scheme 1. Synthesis of Py_6MC2. BRSM: based on recovered starting material.

We began our synthetic endeavors from Py_6MC2 (Scheme 1), expecting that a bulky ethylene glycol side chain might be able to shift the equilibrium to the "closed" conformation and facilitate the ring-closure (Fig. S1). Sonogashira coupling of **4** with **5** gave a pentapyridine oligomer, which was treated with aqueous LiOH [25] to provide mono-deprotected **6**, together with recovered starting material and the bis-deprotected byproduct. The coupling of **6** with 2,6-diiodo-*N*,*N*-dipropylpyridin-4-amine **7** followed by TIPS removal gave a linear hexapyridine oligomer **8**, whose cyclization was initially attempted using classical Sonogashira catalysts $PdCl_2(PPh_3)_2$ and CuI under *pseudo*-high-dilution conditions. The formation of Py_6MC2 was observed by mass spectrometry, yet its isolation was complicated by the low yield (8 %). We accidentally found that a stoichiometric amount of CuI (relative to **8**) improved the reaction and furnished Py_6MC2 in 21 % yield. This contradicted the traditional wisdom that Cu accelerates the alkyne homocoupling side reaction [26–28]. Meanwhile, a higher yield of 33 % was achieved by a copper-free Sonogashira cyclization [29–31] with $Pd(PPh_3)_4$ as the sole catalyst and K_2CO_3 as an additive (Table S1). Py_6MC1 and Py_6MC3 were prepared under similar conditions (Schemes S4 and S5 in Supporting information). The structures of all three macrocycles were determined unambiguously by single-crystal X-ray diffraction. Py_6MC1 and Py_6MC2 were also characterized by NMR spectroscopy and mass spectrometry. The low solubility of Py_6MC3 in common organic solvents precluded characterizations other than mass spectroscopy.

Single crystals of Py_6MC1 and Py_6MC2 were both obtained by slow evaporation of their acetonitrile solutions. Py_6MC1 crystallized in a triclinic *P*-1 space group, with two macrocycles and four CH_3CN in a unit cell. As shown in Fig. 2a, one molecule of Py_6MC1 (yellow) is a planar hexagon, while the other (green) adopts a non-planar chair-like conformation. Each macrocycle cavity hosts two triethylene glycol (Tg) side chains of neighboring macrocycles. The polar C–H bonds of Tg form C–H···N hydrogen bonds (2.6–2.7 Å) with nitrogen atoms of the pyridines. We also observed parallel-displaced stacking of the pyridine-acetylene-pyridine "edges" of adjacent hexagons, at pyridine-pyridine (centroid-to-centroid) distance of 3.6–3.8 Å. Each Py_6MC1 interacts with six neighboring macrocycles, three on the top and bottom sides each (Fig. 2b). Py_6MC2 crystallized in a triclinic *P*-1 space group, with one macrocycle and four CH_3CN per unit cell. The macrocycle adopts a non-planar chair-like conformation, with the two pyridine rings deviating by 11.4° and 20.1° from the central plane, respectively (Fig. 2c). The pyridine-pyridine stacking is weak with an average distance of 3.8 Å. Similar to Py_6MC1, C–H···N hydrogen bonds (2.6–2.7 Å) between Tg and pyridine were observed. Two adjacent macrocycles form a slipped head-to-head dimer, allowing the cavity to host the Tg side chains of each other (Fig. 2d). Crystals of Py_6MC3 were obtained fortuitously by slow evaporation of a THF solution despite its low solubility. Its structure was solved in an orthorhombic $Pna2_1$ space group, with one macrocycle and 10 water molecules per unit cell. Py_6MC3 adopts a boat-like conformation (Fig. 2e), with two pyridines bent upwards by 26.0° and 28.9° from the central plane. The $(H_2O)_{10}$ cluster is partially buried within the cavity, forming three strong O–H···N hydrogen bonds (2.1 Å) with pyridines, in addition to eleven hydrogen bonds among water molecules. Since no water was added during crystallization, they were likely captured from the air. Each Py_6MC3 is in contact with four neighboring macrocycles, two through pyridine-pyridine stacking (3.6–3.8 Å), and the other two through geometrical complementarity (Fig. 2f).

Taken together, the crystal structures of Py_6MC1–3 suggest these macrocycles can adopt planar as well as distorted non-planar conformations. We also concluded that their cavities are highly polar, with strong affinity towards Tg side chains or water molecules. Both features suggest that Py_6MCs can serve as excellent supramolecular hosts for polar guests.

Photophysical properties of the macrocycles were subsequently investigated. Their UV–vis absorption spectra in THF were almost identical, with prominent bands between 280 nm and 350 nm (Fig. 3a). Py_6MC1 and Py_6MC3 exhibited similar emission features, with maximum emission peaks at 337 and 341 nm, respectively. The Stokes shifts (17 nm and 21 nm) were relatively small, consistent with their rigid macrocyclic structures. The emission spectrum of Py_6MC2 showed a small shoulder peak at 343 nm, and a red-shifted broad peak centered at 418 nm, likely a result of excimer-like emission [32]. This conjecture was supported by the presence of a strong "monomer" band at 346 nm and a weaker "excimer" band at 438 nm in CH_3CN (Fig. 3b). Similarly, two emission bands were observed for Py_6MC2 in MeOH, with the monomer band at a lower intensity. Increasing the temperature or addition of water to a THF solution led to enhanced monomer band and weakened excimer band (Figs. S65 and S66 in Supporting information). All evidences agreed with the formation of a Py_6MC2 excimer similar to the solid-state dimer (Fig. 2c).

Given the polar and electron-rich cavities of Py_6MCs, we explored their supramolecular interaction with cationic guests, including two moderately sized *N*-methyl pyridinium derivatives **G1** and **G2**, four quaternary ammonium cations of moderate

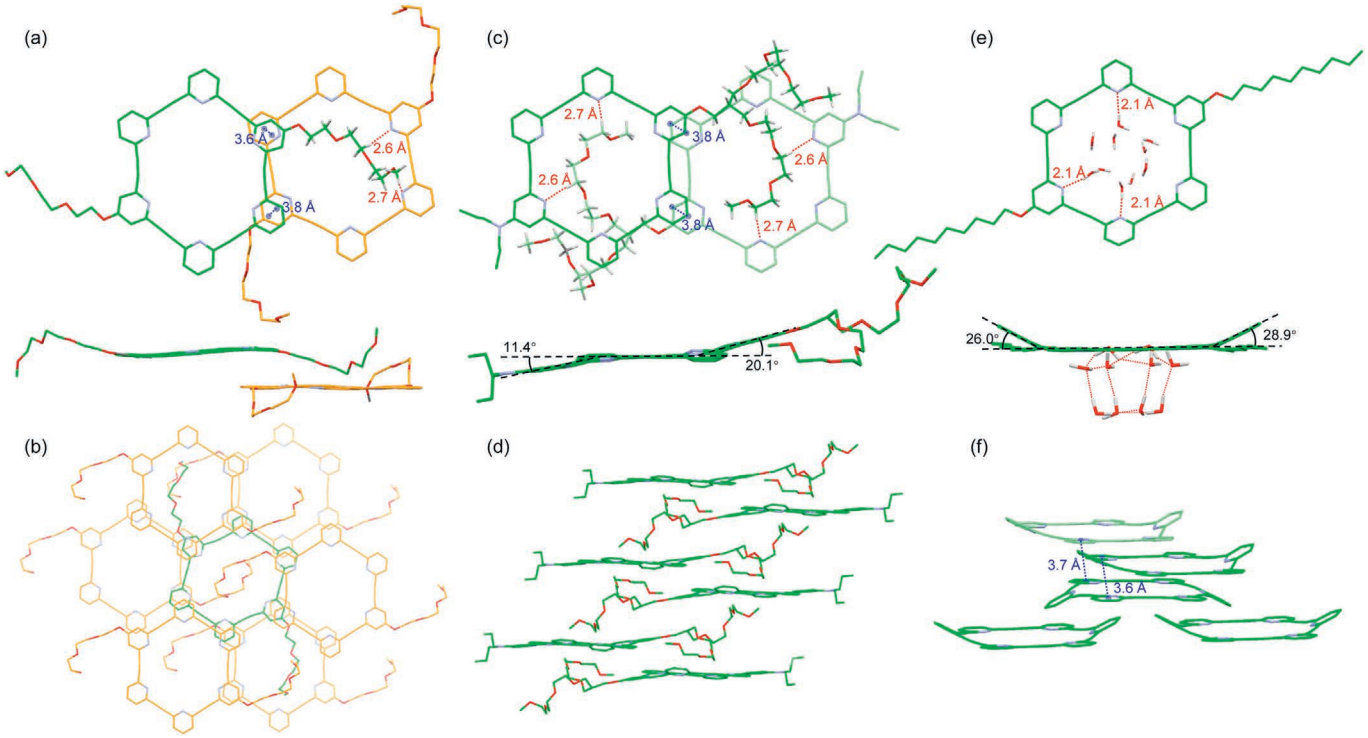


Fig. 2. Crystal structures of Py_6MC1–3. Solvents and hydrogen atoms were partially omitted for clarity. (a) Top and side views of a unit cell of Py_6MC1 and (b) its packing diagram. (c) Top view (dimer) and side view of Py_6MC2 and (d) its packing diagram. (e) Top and side views of Py_6MC3 and the bound water cluster and (f) the packing diagram of Py_6MC3 with side chains omitted. The crystallographic data are available from the Cambridge Crystallographic Data Centre (CCDC) under deposition numbers 2500515–2500517.

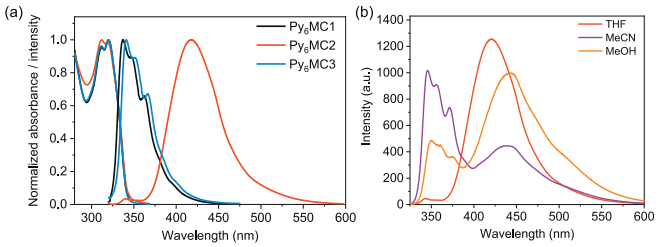


Fig. 3. (a) Normalized UV–vis and fluorescence emission spectra of Py_6MC1–3 in THF ($\lambda_{ex} = 310$ nm, 298 K). (b) Fluorescence emission spectra of Py_6MC2 in THF, CH_3CN, and CH_3OH. Macrocycle concentration at 10 μmol/L.

(**G3**, **G4**) and large (**G5**, **G6**) size, and cations of two pharmaceutical agents-Neostigmine **G7** [33] and Pancuronium **G8** [34] (Fig. 4a). ^{1}H NMR experiments were carried out for qualitative studies, and Py_6MC2 was used as a host for its high solubility. Upon mixing equimolar amounts of Py_6MC2 and the tetrakis[3,5-bis(trifluoromethyl)phenyl]borate (BArF) salt of **G1** in $CDCl_3$, notable changes were observed for NMR signals of both the host and the guest (Fig. 4b). Protons H^1, H^2, and H^3 all exhibited pronounced downfield shifts ($\Delta\delta = 0.91$, 1.25, 0.89 ppm, respectively). Proton H^4, which was distant from the cationic N center, also exhibited downfield shift of 0.52 ppm. These suggested strong host-guest interaction, with **G1** residing inside the cavity and its protons deshielded due to C–H···N hydrogen bonds, or analogous weak interactions. Meanwhile, pyridine protons of Py_6MC2 showed downfield shifts (0.08–0.11 ppm), due to the through-space deshielding by cation **G1**. Similar chemical shift changes were observed for protons of substituted (H^d and H^e) and unsubstituted (H^f and H^g) pyridines, likely due to fast rotation of **G1** inside the macrocycle cavity. The Job plots obtained from ^{1}H NMR measurements revealed a 1:1 binding mode (Fig. 4c).

The interactions between Py_6MC2 and **G2-G8** were studied under identical conditions, and significant chemical shift changes were observed for all guests (Table S4 in Supporting information). The methyl (1.05 ppm) and aromatic (1.27–1.53 ppm) protons of **G2** experienced larger downfield shifts than those of **G1**, indicating that the smaller **G2** is also tightly captured. While **G3** and **G4** appeared to be too large to fit in the cavity, they also had strong interactions with Py_6MC2. For **G3**, the change of chemical shift of methyl protons H^1 (0.60 ppm) was smaller than that of **G1**, suggesting reduced hydrogen-bonding capability. Its aromatic protons H^2-H^4 showed progressively decreasing downfield shifts (0.67, 0.30, and 0.23 ppm, respectively) with increasing distance from the cationic N center. The methyl protons H^1 of **G4** exhibited large downfield shifts (0.72 ppm), while smaller changes were observed for protons H^2 (0.44 ppm) and H^3 (0.10 ppm) of less polarized C–H bonds. The same trend was observed for **G5**, whose protons H^1-H^3 showed decreasing downfield shifts (0.58, 0.40, and 0.07 ppm, respectively). The presence of one set of signals also suggested conformational freedom of **G5** in the host-guest complex. **G6** is similar to **G5** in size but with a rod-like geometry instead. Protons H^1-H^3 of **G6** exhibited downfield shifts (0.39, 0.56, and 0.16 ppm, respectively), while aromatic protons H^4 and H^5 experienced upfield shifts (-0.07 and -0.09 ppm). These peculiar results might stem from π-π interactions between the phenyl group of **G6** and pyridines of the host. **G7** is an analog of **G3** with an additional *N,N*-dimethylaminoacyloxy group at the *meta*-position. The change of chemical shifts of most **G7** protons were comparable to those of **G3** (0.21–0.78 ppm), while the amide methyl protons experienced upfield shifts (-0.28 ppm) due to the shielding effect of pyridines. The bulky **G8** also engaged in strong host-guest interaction with significant chemical shift changes. The *N*-methyl protons H^1 and H^2 exhibited downfield shifts (0.17 and 0.27 ppm), while H^3-H^6 showed upfield shifts (-0.07, -0.09, -0.09 and -0.05 ppm, respectively). It is

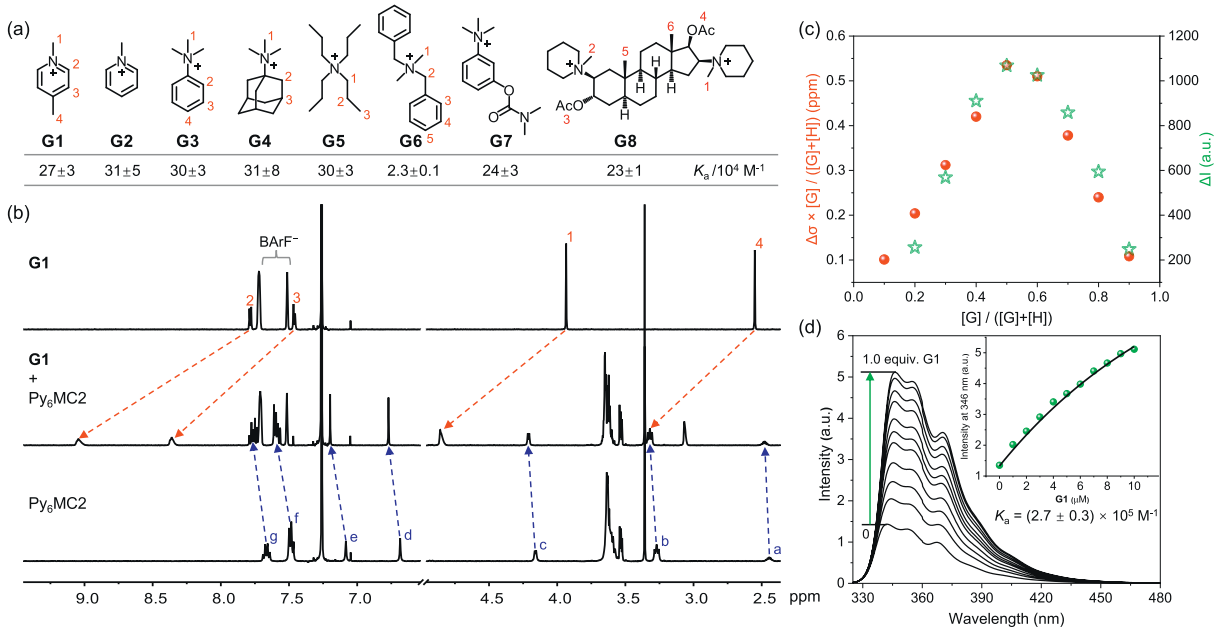


Fig. 4. (a) Guests **G1**–**G8** and corresponding K_a values with Py_6MC1. (b) Partial ^1H NMR spectra (1.0 mmol/L, 500 MHz, $CDCl_3$, 298 K) of **G1**, Py_6MC2·**G1**, and Py_6MC2. (c) The Job plots of host-guest interactions obtained by ^1H NMR (red dots) and fluorescence (green stars) titration experiments. (d) Fluorometric titration spectra of Py_6MC1 (10 μmol/L in THF) with **G1**. Inset: titration data fitted using a 1:1 binding model.

likely that **G8** formed a threaded pseudo rotaxane complex with Py_6MC2.

Fluorescence titrations were carried out to quantify host-guest interactions. Owing to the complex fluorescence behavior of Py_6MC2, the association constant K_a was determined using Py_6MC1 as the host. As shown in Fig. 4d, upon addition of **G1**, a steady increase in fluorescence intensity was observed, which was attributed to the restricted conformation of Py_6MC1 in the host-guest complex. The Job plots (Fig. 4c) confirmed the 1:1 binding mode, and K_a was determined to be $(2.7 \pm 0.3) \times 10^5$ L/mol [35]. Similar increases of fluorescence were observed upon titration of Py_6MC1 with **G2**-**G8** (Figs. S75-S81 in Supporting information), and high K_a values (2.3-3.1 $\times 10^5$ L/mol) were obtained for all guests except **G6**, despite their different sizes and shapes. The binding affinity of Py_6MCs towards cationic guests is comparable to Cai's arene [36] and Li's BINOL[2]arene [37], and slightly higher than Chen's helic[6]arene [38]. This highlights the potential of endo-functionalized shape-persistent macrocycles as supramolecular hosts. In addition, the high binding affinity for **G7** and **G8** makes Py_6MCs relevant in biomedicine [39,40].

DFT calculation was performed on complexes Py_6MC·**G1**–**8**. The optimized structures showed that cationic guests indeed reside in the cavity, and the macrocycle experienced different levels of distortion as a result of cation-binding (Fig. 5a). Py_6MC remains largely planar in Py_6MC·**G1** as **G1** fits well with the cavity, and independent gradient model (IGM) analysis [41] highlighted the stabilizing C–H···N and C–H···π_{alkyne} interactions (Fig. 5b). The adaptivity of Py_6MC allows for strong binding of a smaller guest **G2** and a larger guest **G3**. Py_6MC adopted a distorted boat-like conformation to accommodate sterically demanding **G4**, with the adamantyl moiety was partially buried in the cavity. The alkyl chains of **G5** were fully extended, and Py_6MC was distorted to maximize C–H···N interactions. In contrast, the conformation of **G6** was restricted due to phenyl-pyridine π_{Ph}-π_{Py} interactions, which led to diminished electrostatic host-guest interactions. This observation is consistent with the smaller K_a of 2.3×10^4 L/mol for **G6** compared to other guests. Py_6MC adopted more distorted conformation upon binding **G7** compared to **G3**, which is likely compensated by C–H···π_{Py} interactions as comparable K_a were obtained for both guests. The Py_6MC·**G8** complex showed that the bulky steroid threaded through the cavity, in alignment with the chemical shift changes in ^1H NMR experiments.

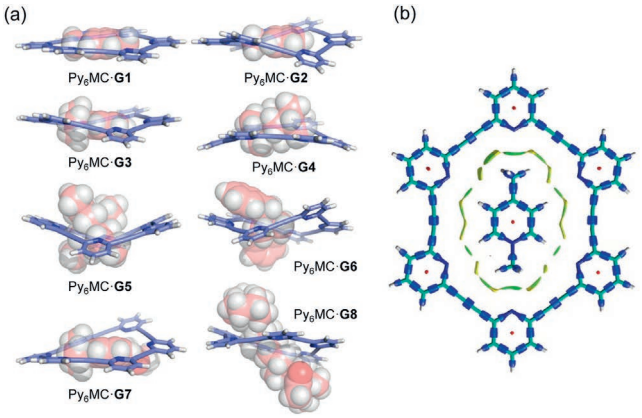


Fig. 5. (a) Energy-minimized structures of Py_6MC·**G1-G8**. (b) Intermolecular binding isosurfaces of complex Py_6MC·**G1** obtained by IGM analysis, with isosurfaces mapped at IRI = 1.1 and $sign(\lambda_2)\rho$ range of -0.04 to +0.02.

Calculation also provided information on the energetic cost of host deformation during binding. The strain energy ΔE is defined as the electronic energy of Py_6MC in the host-guest complex relative to free macrocycle. ΔE was found to be 2.5 and 3.9 kcal/mol for Py_6MC·**G1** and Py_6MC·**G2**, respectively. Surprisingly, the energetic cost was lower for larger guests **G3** (1.3 kcal/mol) and **G4** (1.0 kcal/mol). The ΔE of Py_6MC·**G5** was found to be 4.5 kcal/mol, a result of macrocycle deformation into a "V" shape geometry to maximize C–H···N interactions. Py_6MC·**G6** exhibited the highest ΔE of 5.8 kcal/mol to meet the geometrical requirements for simultaneous π_{Ph}-π_{Py} and C–H···N interactions. The ΔE of Py_6MC·**G7** was 5.2 kcal/mol, which is 3.9 kcal/mol higher than that of **G3**. Only a moderate 4.0 kcal/mol strain was noticed for the pseudo rotaxane complex Py_6MC·**G8**.

In summary, we achieved the effective synthesis of Py_6MCs with a high level of endo-functionalization. Single-crystal X-ray diffraction revealed their conformational flexibility and cavity polarity. The conjugated framework of Py_6MCs endowed them with decent luminescence properties. Strong 1:1 binding with pyridinium and quaternary ammonium cations of various sizes was established by NMR experiments, and binding affinities towards these guests (K_a from 2.4×10^4 L/mol to 3.1×10^5 L/mol) were determined by fluorescence titration. DFT calculations showed that the adaptive structures allow Py_6MCs to interact with guests of different sizes and shapes. These unique features of Py_6MCs highlight the potential of shape-persistent endo-functionalized macrocycles as supramolecular hosts.

Declaration of competing interest

The authors declare that they have no known competing financial interests or personal relationships that could have appeared to influence the work reported in this paper.

CRediT authorship contribution statement

Pengfei Niu: Writing – review & editing, Writing – original draft, Investigation, Data curation. **Jiawei Ma:** Investigation, Conceptualization. **Beijing Zhang:** Visualization, Investigation. **Ziyao Nie:** Investigation. **Haitao Liu:** Investigation. **Yong Liang:** Writing – review & editing, Supervision, Investigation. **Xing Jiang:** Writing – review & editing, Writing – original draft, Project administration, Investigation, Funding acquisition, Conceptualization.

Acknowledgments

This work was supported partially by National Natural Science Foundation of China (No. 22201080), the Recruitment Program of Guangdong (No. 2021QN02C857), and Guangdong Basic and Applied Basic Research Foundation (Nos. 2024A1515012391, 2025A1515010297).

Supplementary materials

Supplementary material associated with this article can be found, in the online version, at doi:10.1016/j.cclet.2026.112429.

References

[1] C.J. Pedersen, J. Am. Chem. Soc. 89 (1967) 2495–2496.
[2] W. Zhang, J.S. Moore, Angew. Chem. Int. Ed. 45 (2006) 4416–4439.
[3] Z. Liu, S.K.M. Nalluri, J.F. Stoddart, Chem. Soc. Rev. 46 (2017) 2459–2478.
[4] F.Y. Chen, W.C. Geng, K. Cai, D.S. Guo, Chin. Chem. Lett. 35 (2024) 109161.
[5] I. Popov, T.H. Chen, S. Belyakov, et al., Chem. Eur. J. 21 (2015) 2750–2754.
[6] G. Liu, S. Guo, L. Liu, et al., J. Org. Chem. 88 (2023) 10171–10179.
[7] S. Li, Q. Liu, L. Mao, et al., Chin. Chem. Lett. 35 (2024) 109791.
[8] Z.H. Song, Y.F. Ma, H. Han, et al., Chem. Eur. J. 31 (2025) e202403271.
[9] L. Adriaenssens, P. Ballester, Chem. Soc. Rev. 42 (2013) 3261–3277.
[10] C.D. Zhao, H. Yao, S.Y. Li, et al., Chin. Chem. Lett. 35 (2024) 108879.
[11] Y. Ohishi, M. Murase, H. Abe, M. Inouye, Org. Lett. 21 (2019) 6202–6207.
[12] M. Dong, X. Liu, Z.Y. Zhang, et al., Chem. Commun. 58 (2022) 2319–2322.
[13] C. Zhai, E.C. Zulueta, A. Mariscal, et al., Chem. Sci. 15 (2024) 19588–19598.
[14] Y. Lu, S.M. Wang, S.S. He, et al., Chem. Sci. 15 (2024) 14791–14797.
[15] Y. Mao, J. Ma, J. Ji, et al., Chin. Chem. Lett. 35 (2024) 109927.
[16] Y. Yamaguchi, S. Kobayashi, S. Miyamura, et al., Angew. Chem. Int. Ed. 43 (2004) 366–369.
[17] J.L. Alonso-Gómez, A. Navarro-Vázquez, M.M. Cid, Chem. Eur. J. 15 (2009) 6495–6503.
[18] S. Castro-Fernández, I.R. Lahoz, A.L. Llamas-Saiz, et al., Org. Lett. 16 (2014) 1136–1139.
[19] H. Abe, K. Ohtani, D. Suzuki, et al., Org. Lett. 16 (2014) 828–831.
[20] Y. Ohishi, J. Chiba, M. Inouye, J. Org. Chem. 87 (2022) 10825–10835.
[21] Y. Tobe, A. Nagano, K. Kawabata, M. Sonoda, K. Naemura, Org. Lett. 2 (2000) 3265–3268.
[22] H. Abe, H. Kurokawa, Y. Chida, M. Inouye, J. Org. Chem. 76 (2011) 309–311.
[23] H. Abe, Y. Chida, H. Kurokawa, M. Inouye, J. Org. Chem. 76 (2011) 3366–3371.
[24] M. Inouye, M. Waki, H. Abe, J. Am. Chem. Soc. 126 (2004) 2022–2027.
[25] T.P. Heffron, T.F. Jamison, Org. Lett. 5 (2003) 2339–2342.
[26] P. Siemsen, R.C. Livingston, F. Diederich, Angew. Chem. Int. Ed. 39 (2000) 2632–2657.
[27] G. Evano, N. Blanchard, M. Toumi, Chem. Rev. 108 (2008) 3054–3131.
[28] D. Wang, J. Li, N. Li, et al., Green Chem. 12 (2010) 45–48.
[29] A. Soheili, J. Albaneze-Walker, J.A. Murry, P.G. Dormer, D.L. Hughes, Org. Lett. 5 (2003) 4191–4194.
[30] C. Torborg, J. Huang, T. Schulz, et al., Chem. Eur. J. 15 (2009) 1329–1336.
[31] M. Gazvoda, M. Virant, B. Pinter, J. Košmrlj, Nat. Commun. 9 (2018) 4814.
[32] C.Y. Wu, Y.N. Gao, Z.H. Zhang, et al., Chin. Chem. Lett. 35 (2024) 109649.
[33] F. Herbstreit, D. Zigrahn, C. Ochterbeck, J. Peters, M. Eikermann, Anesthesiology 113 (2010) 1280–1288.
[34] T. Raghavendra, J. R. Soc. Med. 95 (2002) 363–367.
[35] P. Thordarson, Chem. Soc. Rev. 40 (2011) 1305–1323.
[36] H. Han, R. Fu, R. Wang, et al., J. Am. Chem. Soc. 144 (2022) 20351–20362.
[37] G. Sun, X. Zhang, Z. Zheng, et al., J. Am. Chem. Soc. 146 (2024) 26233–26242.
[38] G.W. Zhang, P.F. Li, H.X. Wang, Y. Han, C.F. Chen, Chem. Eur. J. 23 (2017) 3735–3742.
[39] H.K. Liu, F. Lin, S.B. Yu, et al., J. Med. Chem. 65 (2022) 16893–16901.
[40] Y. Zhao, L. Chen, J. Chen, et al., Chem. Commun. 59 (2023) 5858–5861.
[41] T. Lu, Q. Chen, Chem. Methods 1 (2021) 231–239.